

10-6-2008

Theoretical Top Quark Cross Section at the Fermilab Tevatron and the CERN LHC


Nikolaos Kidonakis

Kennesaw State University, nkidonak@kennesaw.edu

Ramona Vogt

University of California - Davis

Follow this and additional works at: <https://digitalcommons.kennesaw.edu/facpubs>

 Part of the [Atomic, Molecular and Optical Physics Commons](#), [Elementary Particles and Fields and String Theory Commons](#), and the [Nuclear Commons](#)

Recommended Citation

Kidonakis N and Vogt R. 2008. Theoretical top quark cross section at the fermilab tevatron and the CERN LHC. Phys Rev D 78(7):074005.

This Article is brought to you for free and open access by DigitalCommons@Kennesaw State University. It has been accepted for inclusion in Faculty Publications by an authorized administrator of DigitalCommons@Kennesaw State University. For more information, please contact digitalcommons@kennesaw.edu.

The theoretical top quark cross section at the Tevatron and the LHC

Nikolaos Kidonakis⁽¹⁾ and Ramona Vogt^(2,3)

⁽¹⁾*Kennesaw State University, Physics #1202
1000 Chastain Rd., Kennesaw, GA 30144-5591, USA*

⁽²⁾*Lawrence Livermore National Laboratory
Livermore, CA 94551, USA*

⁽³⁾*Physics Department, University of California at Davis
Davis, CA 95616, USA*

Abstract

We present results for the top quark pair cross section at the Tevatron and the LHC. We use the resummed double differential cross section, employing the fully kinematics-dependent soft anomalous dimension matrices, to calculate the soft-gluon contributions at next-to-next-to-leading order (NNLO). We improve and update our previous estimates by refining our methods, including further subleading terms, and employing the most recent parton distribution function sets. The NNLO soft corrections significantly enhance the NLO cross section while considerably reducing the scale dependence. We provide a detailed discussion of all theoretical uncertainties in our calculation, including kinematics, scale, and parton distributions uncertainties and clarify the differences between our work and other approaches in the literature.

1 Introduction

The top quark holds a special place in the Standard Model of particle physics as the heaviest elementary particle. Since the discovery of the top quark via $t\bar{t}$ production in proton-antiproton collisions at the Tevatron [1] its mass [2] and production cross section [3, 4] have been determined with increasing accuracy. There is also now evidence for single-top production at the Tevatron [5]. At the LHC, both the $t\bar{t}$ and single top production cross sections will be two orders of magnitude higher than at the Tevatron. For recent reviews of top quark physics in hadron colliders see [6].

The top quark cross section receives large corrections from soft-gluon contributions near threshold which can be formally resummed. The resummation at next-to-leading logarithmic (NLL) accuracy for hard scattering cross sections and, in particular, top quark pair production was performed in Ref. [7]. (For recent results on single top production, see Ref. [8]). To achieve such accuracy, it is necessary to derive the soft anomalous dimension matrix, which controls noncollinear soft-gluon emission, to one loop. At NLL the color structure of the hard scattering enters in a non-trivial way and each partonic process has to be treated separately. The soft anomalous dimension matrix is dependent on all the kinematical variables. Thus this is a fully differential calculation which can be applied to total cross sections as well as to differential cross sections, such as transverse momentum and rapidity distributions.

Later, another formalism [9] was proposed for the total cross section only. This calculationally simpler approach does not, however, involve the exact differential kinematics and instead makes the approximation that the NNLO and NLO rapidity dependence is the same. Hence, numerical deviations from the exact kinematics-sensitive result can appear. (For a detailed discussion and a numerical comparison in the context of direct photon production, see Ref. [10]).

In Refs. [7, 9], the resummation is performed in moment space. Since the expression for the resummed cross section diverges at the Landau pole, a prescription is needed to define the physical resummed cross section when inverting from moment to momentum space. Alternatively, to avoid prescription dependence, the resummed cross section can be expanded to NNLO or higher orders.

The formalism of Ref. [7] was used in detailed phenomenological studies [11, 12] where NNLO expansions were provided at NNLL accuracy, after matching with the complete NLO cross section. Results were provided in both single-particle-inclusive (1PI) and pair-invariant-mass (PIM) kinematics. The kinematics ambiguity was found to be an important source of uncertainty. In 1PI kinematics the soft logarithms are of the form $[\ln^k(s_4/m^2)/s_4]_+$ with m the top quark mass and s_4 the sum of the Mandelstam invariants, $s_4 = s + t_1 + u_1$. Near threshold, $s_4 \rightarrow 0$. The soft-gluon corrections to the double differential cross section, $d^2\sigma/(dt_1 du_1)$, were calculated. In PIM kinematics, the soft logarithms are of the form $[\ln^k(1-z)/(1-z)]_+$ with $z = M^2/s$, where M^2 is the $t\bar{t}$ pair mass squared. Near threshold, $z \rightarrow 1$. The soft gluon corrections to the double differential cross section, $d^2\sigma/(dM^2 d\cos\theta)$, where θ is the scattering angle in the partonic center-of-mass frame, were calculated. The cross section in PIM kinematics was found to be smaller than the 1PI result. The difference, an uncertainty due to uncalculated terms, was found to be larger than the scale variation. In Ref. [12], results were also given for the exact scale variation at NNLO. The magnitude of this variation was also found to depend

on the kinematics.

The formalism of Ref. [9] was also used to derive NLL resummed numerical results (recently updated [13]) for top pair production at the Tevatron and LHC. The corrections beyond NNLO are negligible [9] (also shown to be small in Ref. [14]); hence the resummed cross section is numerically very similar to the NNLO expansion at the given logarithmic accuracy. However, a minimal prescription was used to define the resummed cross section in Ref. [9] and, as shown in Ref. [11], the differences in the prescription formalism, as well as the treatment of the kinematics, are much bigger than higher order terms at NNNLO and beyond. Hence the results of Ref. [9] are quite different from Refs. [11, 12], both theoretically and numerically.

The approach in Refs. [11, 12] was later improved by adding NNNLL terms at NNLO [15]. Although the complete NNNLL terms require calculation of the two-loop soft anomalous dimension matrix, it was clearly demonstrated [15] that the contribution of this matrix at two loops is expected to be negligible. Thus it is possible to obtain an effective NNNLL calculation by including all other terms. The ζ terms arising from the inversion to momentum space (including some ζ virtual terms) are dominant, as shown by expressing the partonic cross sections in terms of scaling functions that depend on the variable $\eta = s/(4m^2) - 1$ and comparing the 1PI and PIM scaling functions over a large range of η . Since a complete NNLO calculation should be independent of the kinematics, the difference between the 1PI and PIM results as a function of η is an indication of the unknown terms. Away from threshold, hard gluon terms contribute. Since their form is also kinematics dependent it is inevitable that, as one moves away from the threshold region, the 1PI and PIM results diverge. However, near threshold the soft gluons dominate and thus a complete calculation of the soft terms should produce agreement between the 1PI and PIM scaling functions. At NNLL, the 1PI and PIM functions diverge already at threshold [12], indicating that the NNNLL terms are non-negligible. However, when the NNNLL terms were added [15], this discrepancy disappeared, as one would expect when all NNLO soft terms are included. Thus the contribution of the unknown two-loop soft-anomalous-dimension terms that were left out is negligible and we obtain an excellent approximation to the complete NNNLL terms and an effective NNNLL calculation, denoted NNLO-NNNLL+ ζ in Ref. [15].

Recently the two-loop soft anomalous dimension for massless quark scattering was completed [16]. (Work is in progress for heavy quark production [17].) It was shown [16] that the two-loop soft anomalous dimension is simply the one-loop result multiplied by half the two-loop quantity K [18]. Assuming that this relation also holds for heavy quarks, consistent with the two-loop results in Ref. [19], the contribution of this additional two-loop term to the total cross section is less than 1 per mille at both the Tevatron and LHC energies. It is thus insignificant relative to the size of other terms and sources of uncertainty, as expected [15], verifying the robustness of the calculation in Ref. [15].

A very recent paper [19] uses the general approach of Ref. [9], extending the results of Ref. [9] by adding the NNLL terms in the resummed expression. A NNLO expansion in powers of $\ln \beta$, where $\beta = \sqrt{1 - 4m^2/s}$, is also presented in Ref. [19]. An additional two-loop term is also included, a rough analog of the two-loop soft anomalous dimension term in the formalism of Refs. [7, 16, 17]. This two-loop term is again given by the one-loop result multiplied by the two-loop quantity K [18], analogous to the result of Ref. [16]. We have investigated the contribution of this two-loop term within the approach of Ref. [19] and find it to be numerically

negligible, on the order of a few per mille, consistent with the study mentioned previously and again verifying that this two-loop contribution is numerically insignificant. Since [19] uses the formalism and approximation of Ref. [9], their results differ from ours for the reasons explained earlier. We use exact kinematics in a double differential cross section and define partonic threshold through the quantities s_4 or z , depending on the kinematics choice, while Ref. [19] defines threshold at the total cross section level only in terms of β .

We also note that the authors of Ref. [19] use the exact scale dependence of the NNLO cross section, finding a smaller scale dependence than in Refs. [9, 13]. The exact NNLO scale dependence was first calculated in Ref. [12] and shown to crucially depend on the kinematics choice (1PI or PIM). Hence the scale variation in Refs. [9, 19] cannot be directly compared with that of Ref. [12] or the present paper.

We also find it more consistent to use the same level of accuracy for the scale-dependent terms as for the other terms in the calculation, also chosen for the final results in Refs. [12, 15]. We obtain a smaller scale dependence at the Tevatron than Ref. [19] but a larger one at the LHC. In our approach, the kinematics ambiguity is bigger than the scale variation at the Tevatron but smaller at the LHC. The results in Refs. [9, 13, 19] do not have a kinematics uncertainty because their approximation is insensitive to the kinematics choice. Therefore the scale dependence in those approaches, in particular the small scale uncertainty at the LHC of Ref. [19], is not necessarily indicative of the true theoretical uncertainty in the cross section.

In Ref. [19] subleading Coulomb terms, calculated in [20], were included in the numerical results. In Ref. [15] some, but not all, of these terms were included. We find that these additional contributions are completely negligible at the Tevatron, and make a very small contribution, included in our new results, at the LHC.

In this paper, we present detailed results for the top quark cross section at the Tevatron and the LHC. We primarily use the theoretical approach of Ref. [15] with some changes and refinements, described in the text, along with the newest available parton distribution functions (PDFs). We also provide a detailed study of theoretical uncertainties including kinematics, scale, and PDF uncertainties, as well as a discussion of other sources. In Section 2 we provide results for the $t\bar{t}$ production cross section in $p\bar{p}$ collisions at the Tevatron at $\sqrt{S} = 1.96$ TeV. In Section 3 we give the $t\bar{t}$ production cross section in pp collisions at the LHC at $\sqrt{S} = 14$ TeV as well as a prediction for 10 TeV.

2 The top quark cross section at the Tevatron

We begin with $t\bar{t}$ production at the Tevatron at $\sqrt{S} = 1.96$ TeV. The leading-order partonic processes are $q\bar{q} \rightarrow t\bar{t}$ and $gg \rightarrow t\bar{t}$. In $p\bar{p}$ collisions at the Tevatron, the $q\bar{q}$ channel is dominant. In addition to corrections to the LO processes, at NLO there are small contributions from two additional processes, qg and $\bar{q}g$.

We first calculate the NLO cross section [21], including all channels. We then add the NNLO soft-gluon corrections in the $q\bar{q}$ and gg channels to the NLO result. We calculate the soft-gluon corrections in both 1PI and PIM kinematics. We find that the behavior of the $q\bar{q} \rightarrow t\bar{t}$ and $gg \rightarrow t\bar{t}$ contributions is quite different. The $q\bar{q}$ channel, with only one diagram at LO, is well behaved in both kinematics. The gg channel is, however, better treated in 1PI kinematics

because the three LO $gg \rightarrow t\bar{t}$ diagrams favor 1PI kinematics. In addition, in PIM kinematics the one-loop expansion of the resummed gg cross section is very different from the exact NLO result while the 1PI expansion of the gg contribution is an excellent approximation to the exact NLO result at both the Tevatron and the LHC. Therefore, for our best prediction of the NNLO corrections, we take the average of the 1PI and PIM $q\bar{q}$ soft-gluon corrections and add it to the 1PI gg soft-gluon result. This is a refinement of our previous method [15] where we averaged the 1PI and PIM results from both channels. Our new approach results in a slightly larger total cross section with a somewhat reduced kinematics uncertainty at the Tevatron than in Ref. [15]. As discussed in the Introduction, the effect of the two-loop soft anomalous dimension matrix and further subleading Coulomb terms is negligible with no change on the results presented here.

We present two tables with NLO and approximate NNLO cross sections using the MRST 2006 NNLO [22] and CTEQ6.6M [23] parton densities. While the NNLO approximate cross section is of the same logarithmic accuracy as the NNLO-NNLL+ ζ cross section of Ref. [15], they differ slightly because of the changes and refinements discussed above. All the results are in the $\overline{\text{MS}}$ scheme.

MRST 2006 NNLO		
Mass (GeV)	$\sigma(\text{NLO} \pm \text{scale} \pm \text{PDF})$ (pb)	$\sigma(\text{NNLO approx} \pm \text{kinematics} \pm \text{scale} \pm \text{PDF})$ (pb)
165	9.23 ^{+0.59 +0.27} _{-1.09 -0.23}	9.80 \pm 0.38 ^{+0.04 +0.29} _{-0.34 -0.25}
166	8.93 ^{+0.57 +0.27} _{-1.06 -0.22}	9.48 \pm 0.37 ^{+0.04 +0.29} _{-0.33 -0.24}
167	8.65 ^{+0.55 +0.26} _{-1.02 -0.21}	9.17 \pm 0.36 ^{+0.04 +0.28} _{-0.32 -0.22}
168	8.37 ^{+0.53 +0.25} _{-0.99 -0.20}	8.88 \pm 0.35 ^{+0.04 +0.27} _{-0.31 -0.21}
169	8.11 ^{+0.51 +0.24} _{-0.96 -0.19}	8.60 \pm 0.34 ^{+0.03 +0.26} _{-0.30 -0.20}
170	7.85 ^{+0.50 +0.23} _{-0.93 -0.19}	8.32 \pm 0.33 ^{+0.03 +0.25} _{-0.29 -0.20}
171	7.60 ^{+0.48 +0.23} _{-0.90 -0.18}	8.06 \pm 0.32 ^{+0.03 +0.24} _{-0.28 -0.19}
172	7.36 ^{+0.46 +0.22} _{-0.87 -0.18}	7.80 \pm 0.31 ^{+0.03 +0.23} _{-0.27 -0.19}
173	7.13 ^{+0.45 +0.21} _{-0.84 -0.17}	7.56 \pm 0.30 ^{+0.02 +0.22} _{-0.26 -0.18}
174	6.91 ^{+0.44 +0.20} _{-0.82 -0.17}	7.32 \pm 0.29 ^{+0.02 +0.21} _{-0.26 -0.18}
175	6.70 ^{+0.42 +0.19} _{-0.79 -0.16}	7.09 \pm 0.28 ^{+0.02 +0.20} _{-0.25 -0.17}
176	6.49 ^{+0.41 +0.19} _{-0.77 -0.15}	6.87 \pm 0.27 ^{+0.02 +0.20} _{-0.24 -0.16}
177	6.29 ^{+0.39 +0.18} _{-0.74 -0.15}	6.66 \pm 0.26 ^{+0.02 +0.19} _{-0.23 -0.16}
178	6.10 ^{+0.38 +0.18} _{-0.72 -0.14}	6.46 \pm 0.26 ^{+0.02 +0.19} _{-0.23 -0.15}
179	5.91 ^{+0.37 +0.17} _{-0.70 -0.14}	6.26 \pm 0.25 ^{+0.02 +0.18} _{-0.22 -0.15}
180	5.73 ^{+0.36 +0.17} _{-0.68 -0.13}	6.07 \pm 0.24 ^{+0.01 +0.18} _{-0.21 -0.14}

Table 1: The $t\bar{t}$ production cross section in $p\bar{p}$ collisions at the Tevatron with $\sqrt{S} = 1.96$ TeV using the MRST 2006 NNLO PDFs. The exact NLO results are shown with the scale and PDF uncertainties while the approximate NNLO results include kinematics, scale, and PDF uncertainties.

Table 1 provides the $p\bar{p} \rightarrow t\bar{t}$ cross section for $165 < m < 180$ GeV, in 1 GeV increments

calculated with the MRST 2006 NNLO PDFs. We give both the exact NLO and the approximate NNLO cross sections. The central values are calculated with the factorization scale, μ_F , and the renormalization scale, μ_R , set equal to the top quark mass, $\mu_F = \mu_R = \mu = m$, using the central MRST 2006 NNLO PDF.

In addition to the central value of the NLO cross section, we also provide uncertainties due to the scale and PDF variations. The scale is varied over $m/2 < \mu < 2m$. Varying the scale by a factor of two around $\mu = m$ is a standard but arbitrary way to estimate uncertainties from higher-order terms. The + (−) indicates the difference between the calculation with $\mu = m/2$ ($\mu = 2m$) and the central value with $\mu = m$. The PDF uncertainty, calculated using the 30 different MRST 2006 NNLO eigensets, is relatively large, reflecting the uncertainty in the large x region of the PDFs.

The central value of the NNLO approximate cross section is followed by the kinematics uncertainty, the scale variation and the PDF uncertainty. The NNLO scale and PDF uncertainties are obtained the same way as for the NLO cross section. The kinematics uncertainty resides in the treatment of the $q\bar{q}$ channel because the gg channel is only calculated in 1PI kinematics. The central value is obtained from the average of the 1PI and PIM $q\bar{q}$ calculations. The + kinematics uncertainty is the found by taking the 1PI $q\bar{q}$ result alone while the − results uses the PIM $q\bar{q}$ calculation. The kinematics uncertainty is symmetric because the central $q\bar{q}$ contribution is the average of the 1PI and PIM results.

At NLO, the scale variation is significant. When the NNLO corrections are added, the scale dependence on the scale decreases dramatically. However, the kinematics uncertainty is larger than the scale variation. The PDF uncertainty is also significant at NLO and NNLO, of the same order as the kinematics dependence at NNLO.

Table 2 provides the $t\bar{t}$ cross section for $165 < m < 180$ GeV, in 1 GeV increments, using the CTEQ6.6M NLO PDFs. As in Table 1, we list both the exact NLO and our approximate NNLO cross sections together with all uncertainties. The central values, again shown with $\mu_F = \mu_R = \mu = m$, employ the central CTEQ6.6M PDFs.

The scale variation is calculated as described above for the MRST 2006 NNLO PDFs. In the case of the NNLO approximate cross section, the NNLO results at both ends of the scale range, $\mu = m/2$ and $2m$, are lower than with $\mu = m$, indicated by the double minus signs on the scale uncertainty. The PDF uncertainty is calculated using the 44 different CTEQ6.6M eigensets.

The two sets of results are quite different. The cross sections calculated with CTEQ6.6M are smaller than those with the central MRST 2006 NNLO set but have larger PDF uncertainties. Indeed, the CTEQ6.6M NNLO approximate cross sections are quite similar to the NLO cross section calculated with the MRST 2006 NNLO PDFs. Part of the difference can be attributed to the fact that the MRST 2006 NNLO sets are of the same order as the NNLO approximate calculation while the CTEQ6.6M sets are NLO. Furthermore, the CTEQ6.6M large- x gluon distribution is smaller, reducing the relative gg contribution.

The best way to combine the uncertainties is not obvious. The most conservative approach would be to add them linearly. However the kinematics and scale uncertainties both reflect the neglect of unknown terms. Thus a linear combination of the uncertainties likely provides an overestimate of the overall uncertainty and we instead prefer to add them in quadrature.

We present the NNLO approximate cross section for the current most likely value of the top

CTEQ6.6M		
Mass (GeV)	$\sigma(\text{NLO} \pm \text{scale} \pm \text{PDF})$ (pb)	$\sigma(\text{NNLO approx} \pm \text{kinematics} \pm \text{scale} \pm \text{PDF})$ (pb)
165	8.74 ^{+0.46} _{-0.96} ^{+0.58} _{-0.45}	9.23 \pm 0.37 ^{-0.03} _{-0.25} ^{+0.61} _{-0.48}
166	8.47 ^{+0.44} _{-0.93} ^{+0.56} _{-0.43}	8.93 \pm 0.36 ^{-0.03} _{-0.24} ^{+0.59} _{-0.45}
167	8.20 ^{+0.43} _{-0.90} ^{+0.53} _{-0.42}	8.65 \pm 0.35 ^{-0.03} _{-0.23} ^{+0.56} _{-0.44}
168	7.94 ^{+0.42} _{-0.87} ^{+0.52} _{-0.41}	8.38 \pm 0.34 ^{-0.03} _{-0.23} ^{+0.55} _{-0.43}
169	7.70 ^{+0.40} _{-0.84} ^{+0.50} _{-0.39}	8.12 \pm 0.33 ^{-0.03} _{-0.22} ^{+0.53} _{-0.41}
170	7.46 ^{+0.39} _{-0.82} ^{+0.48} _{-0.38}	7.87 \pm 0.32 ^{-0.03} _{-0.21} ^{+0.51} _{-0.40}
171	7.23 ^{+0.38} _{-0.79} ^{+0.47} _{-0.36}	7.62 \pm 0.31 ^{-0.03} _{-0.21} ^{+0.50} _{-0.38}
172	7.01 ^{+0.37} _{-0.77} ^{+0.45} _{-0.35}	7.39 \pm 0.30 ^{-0.03} _{-0.20} ^{+0.48} _{-0.37}
173	6.79 ^{+0.35} _{-0.74} ^{+0.43} _{-0.34}	7.16 \pm 0.29 ^{-0.03} _{-0.19} ^{+0.45} _{-0.36}
174	6.58 ^{+0.34} _{-0.72} ^{+0.42} _{-0.33}	6.94 \pm 0.28 ^{-0.03} _{-0.19} ^{+0.44} _{-0.35}
175	6.38 ^{+0.33} _{-0.70} ^{+0.41} _{-0.31}	6.73 \pm 0.27 ^{-0.03} _{-0.18} ^{+0.43} _{-0.33}
176	6.19 ^{+0.32} _{-0.68} ^{+0.39} _{-0.30}	6.53 \pm 0.27 ^{-0.03} _{-0.18} ^{+0.41} _{-0.32}
177	6.00 ^{+0.31} _{-0.66} ^{+0.38} _{-0.29}	6.33 \pm 0.26 ^{-0.03} _{-0.17} ^{+0.40} _{-0.31}
178	5.82 ^{+0.30} _{-0.64} ^{+0.37} _{-0.28}	6.14 \pm 0.25 ^{-0.03} _{-0.17} ^{+0.39} _{-0.30}
179	5.65 ^{+0.29} _{-0.62} ^{+0.35} _{-0.27}	5.95 \pm 0.24 ^{-0.03} _{-0.16} ^{+0.37} _{-0.28}
180	5.48 ^{+0.28} _{-0.60} ^{+0.34} _{-0.26}	5.77 \pm 0.24 ^{-0.03} _{-0.16} ^{+0.36} _{-0.27}

Table 2: The $t\bar{t}$ production cross section in $p\bar{p}$ collisions at the Tevatron with $\sqrt{S} = 1.96$ TeV using the CTEQ6.6M PDFs. The exact NLO results are shown with the scale and PDF uncertainties while the approximate NNLO results include kinematics, scale, and PDF uncertainties.

quark mass, $m = 172$ GeV for both sets of PDFs. We first give the central result from Tables 1 and 2 with all the uncertainties shown separately and then add the uncertainties in quadrature for our final result. Using the MRST 2006 NNLO PDFs, we have

$$\sigma_{p\bar{p} \rightarrow t\bar{t}}^{\text{NNLOapprox}}(1.96 \text{ TeV}, m = 172 \text{ GeV}, \text{MRST}) = 7.80 \pm 0.31 \begin{matrix} +0.03 & +0.23 \\ -0.27 & -0.19 \end{matrix} \text{ pb} = 7.80 \begin{matrix} +0.39 \\ -0.45 \end{matrix} \text{ pb}, \quad (2.1)$$

while with CTEQ6.6M we find

$$\sigma_{p\bar{p} \rightarrow t\bar{t}}^{\text{NNLOapprox}}(1.96 \text{ TeV}, m = 172 \text{ GeV}, \text{CTEQ}) = 7.39 \pm 0.30 \begin{matrix} -0.03 & +0.48 \\ -0.20 & -0.37 \end{matrix} \text{ pb} = 7.39 \begin{matrix} +0.57 \\ -0.52 \end{matrix} \text{ pb}. \quad (2.2)$$

We have not included further theoretical ambiguities arising from the choice of equivalent analytical expressions near threshold or from damping factors [12] as well as from the virtual ζ terms discussed in Ref. [15]. Such ambiguities are partly accounted for in the kinematics and scale uncertainties shown here.

Figure 1 shows the exact NLO and approximate NNLO top quark cross sections as a function of top quark mass at the Tevatron using the MRST 2006 NNLO (left) and CTEQ6.6M (right) PDFs. Three curves are given for each order: a central value with $\mu = m$ and the extremes of the calculated scale dependence with $\mu = m/2$ and $2m$. The region between the upper and lower scales represents the scale variation at each order. We see that the NNLO scale dependence is much diminished relative to NLO. In fact the NNLO curves with $\mu = m/2$ and $\mu = m$ are on

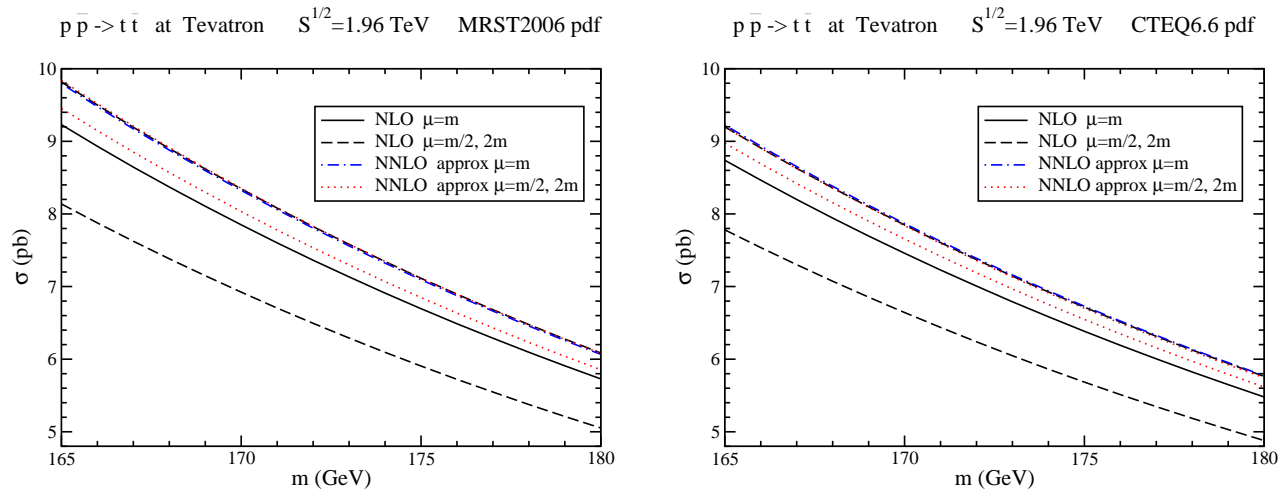


Figure 1: The exact NLO and approximate NNLO cross sections in $p\bar{p}$ collisions at 1.96 TeV using the MRST 2006 NNLO (left) and CTEQ6.6M (right) PDFs.

top of each other as well as on top of the NLO curve with $\mu = m/2$. The kinematics and PDF uncertainties are not represented in the plots.

In Fig. 2, we present the K factors at the Tevatron using the MRST 2006 NNLO (left) and CTEQ6.6M (right) PDFs with our central value, $\mu = m$. The K factors are virtually independent of the PDF although the CTEQ6.6M K factors appear slightly smaller. They are also independent of the top quark mass. The ratios of the approximate NNLO cross sections to the exact LO and NLO cross sections are both given. The NNLO corrections enhance the NLO $t\bar{t}$ cross section by $\sim 6\%$ at $\mu = m$.

3 The top quark cross section at the LHC

We now turn to $t\bar{t}$ production in pp collisions at the LHC. While our results are primarily shown for $\sqrt{S} = 14$ TeV, we also provide predictions for the top quark cross section at the LHC start-up energy of 10 TeV. We note that at the LHC, the gg channel is dominant.

Table 3 provides the top quark cross section for $165 < m < 180$ GeV, in 1 GeV increments, in pp collisions at the LHC with $\sqrt{S} = 14$ TeV employing the MRST 2006 NNLO PDFs. We list both the exact NLO and approximate NNLO cross sections. The central values are given for $\mu_F = \mu_R = \mu = m$ with the central MRST 2006 NNLO PDFs.

The NLO cross section is shown with the uncertainties due to the scale variation and the choice of PDF eigenset. As before, we vary the scale between $\mu = m/2$ and $2m$ and the PDF uncertainty is calculated using the 30 different MRST 2006 NNLO eigensets.

The central value of the NNLO approximate cross section is accompanied by uncertainties due to the kinematics, the scale variation and the choice of PDF. Again, the central value of the approximate NNLO $q\bar{q}$ contribution is the average of the 1PI and PIM kinematics choice. The $+$ ($-$) kinematics uncertainty is the difference between the top cross section with the $q\bar{q}$ contribution calculated in 1PI (PIM) kinematics.

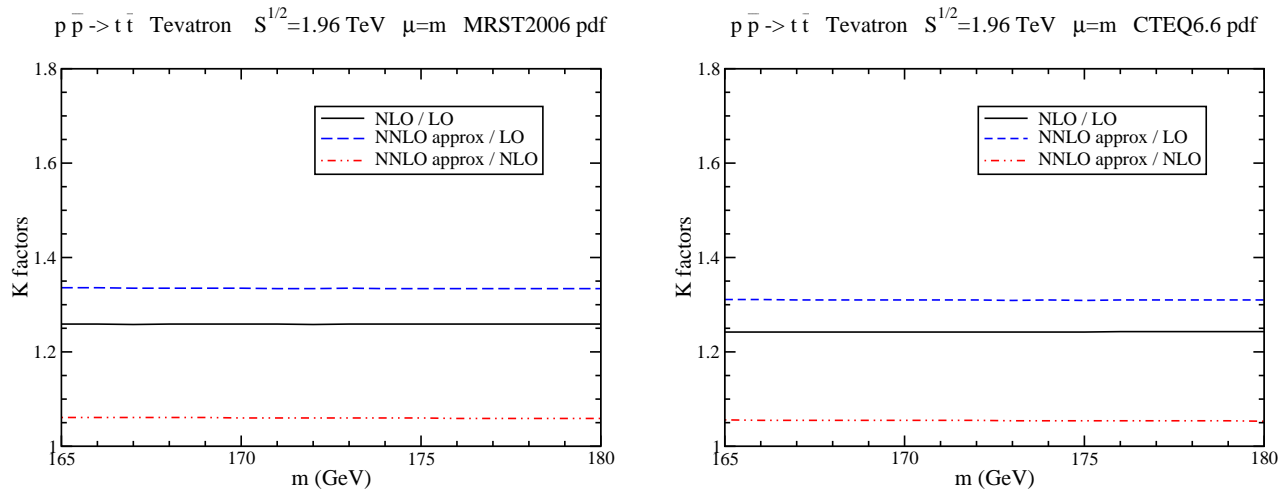


Figure 2: The K factors at the Tevatron using the MRST 2006 NNLO (left) and the CTEQ6.6M (right) PDFs.

At NLO the scale variation is large. When the NNLO corrections are added the dependence on the scale decreases significantly. Now the kinematics uncertainty is much smaller than that due to the scale variation. This is because we only use 1PI kinematics for the gg channel, dominant for pp collisions at this energy. Thus the kinematics uncertainty is only due to the change in the $q\bar{q}$ calculation. The PDF uncertainty is smaller at the LHC since x is relatively small, in a range where the PDFs are better known.

In Table 4, we present the corresponding top cross sections with the CTEQ6.6M NLO PDFs. The CTEQ6.6M results are again smaller than those with the MRST 2006 NNLO sets. While the PDF uncertainty is smaller at the LHC, the CTEQ6.6 uncertainty is still larger than those with MRST 2006 NNLO.

We now present our predicted NNLO approximate cross section for top production in pp collisions at $\sqrt{S} = 14$ TeV with $m = 172$ GeV. The results are again given both with the separate uncertainties, as in Tables 3 and 4, and with uncertainties added in quadrature. Using the MRST 2006 NNLO PDFs, we find

$$\sigma_{pp \rightarrow t\bar{t}}^{\text{NNLOapprox}}(14 \text{ TeV}, m = 172 \text{ GeV}, \text{MRST}) = 968 \pm 4^{+79}_{-50} \pm 12^{+12}_{-13} \text{ pb} = 968^{+80}_{-52} \text{ pb}, \quad (3.1)$$

while with the CTEQ6.6M PDFs, we obtain

$$\sigma_{pp \rightarrow t\bar{t}}^{\text{NNLOapprox}}(14 \text{ TeV}, m = 172 \text{ GeV}, \text{CTEQ}) = 919 \pm 4^{+70}_{-45} \pm 29^{+29}_{-31} \text{ pb} = 919^{+76}_{-55} \text{ pb}. \quad (3.2)$$

Figure 3 shows exact NLO and approximate NNLO top quark cross sections as a function of top quark mass with $\sqrt{S} = 14$ TeV using the MRST 2006 NNLO (left) and CTEQ6.6M (right) PDFs. At each order we show the central result with $\mu = m$ as well as the range of the scale uncertainty indicated by the upper ($\mu = m/2$) and lower ($\mu = 2m$) curves. The region between the upper and lower curves denotes the scale variation. While the NNLO scale dependence is reduced relative to NLO, the reduction is not as large as at the Tevatron. We note that

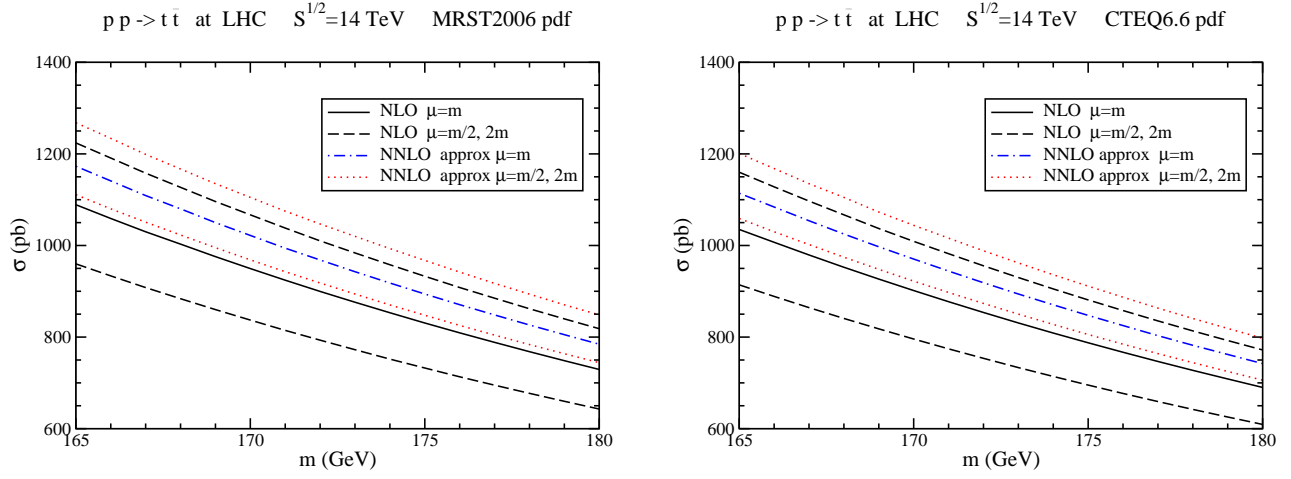


Figure 3: The NLO and approximate NNLO top cross sections in 14 TeV pp collisions at the LHC using the MRST 2006 NNLO (left) and the CTEQ6.6M (right) PDFs.

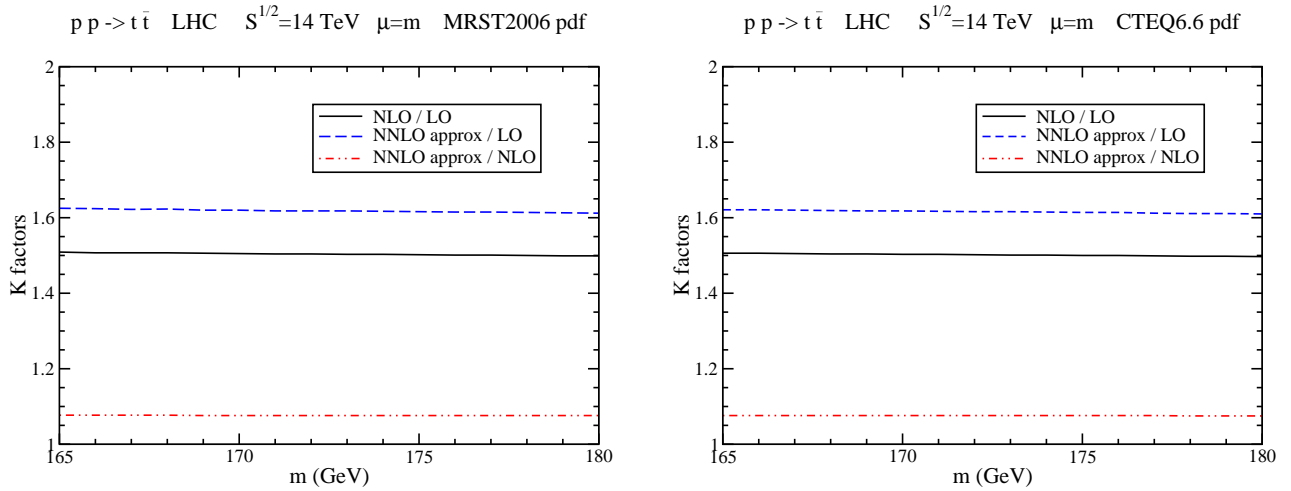


Figure 4: The K factors at the LHC using the MRST 2006 NNLO (left) and CTEQ6.6M (right) PDFs.

MRST 2006 NNLO		
Mass (GeV)	$\sigma(\text{NLO} \pm \text{scale} \pm \text{PDF})$ (pb)	$\sigma(\text{NNLO approx} \pm \text{kinematics} \pm \text{scale} \pm \text{PDF})$ (pb)
165	1089 ^{+135 +12} _{-129 -14}	1173 ± 5 ^{+95 +13} _{-62 -15}
166	1059 ^{+132 +12} _{-125 -13}	1141 ± 5 ^{+93 +13} _{-60 -14}
167	1030 ^{+128 +12} _{-122 -13}	1109 ± 5 ^{+90 +13} _{-58 -14}
168	1003 ^{+124 +12} _{-119 -13}	1080 ± 5 ^{+87 +13} _{-57 -14}
169	976 ^{+120 +12} _{-116 -12}	1050 ± 5 ^{+85 +13} _{-55 -13}
170	950 ^{+117 +12} _{-113 -12}	1022 ± 5 ^{+83 +13} _{-53 -13}
171	924 ^{+114 +12} _{-110 -12}	994 ± 5 ^{+81 +13} _{-52 -13}
172	900 ^{+110 +11} _{-107 -12}	968 ± 4 ^{+79 +12} _{-50 -13}
173	876 ^{+108 +11} _{-104 -11}	943 ± 4 ^{+77 +12} _{-49 -12}
174	853 ^{+105 +11} _{-101 -11}	918 ± 4 ^{+75 +12} _{-48 -12}
175	831 ^{+102 +11} _{-98 -11}	894 ± 4 ^{+73 +12} _{-46 -12}
176	809 ^{+99 +10} _{-96 -10}	871 ± 4 ^{+71 +11} _{-45 -11}
177	788 ^{+97 +10} _{-93 -10}	848 ± 4 ^{+69 +11} _{-44 -11}
178	768 ^{+94 +10} _{-91 -10}	826 ± 4 ^{+67 +11} _{-43 -11}
179	748 ^{+91 +10} _{-89 -10}	805 ± 4 ^{+65 +11} _{-42 -11}
180	729 ^{+89 +9} _{-86 -10}	785 ± 4 ^{+64 +10} _{-40 -11}

Table 3: The $t\bar{t}$ production cross section in pp collisions at the LHC with $\sqrt{S} = 14$ TeV using the MRST 2006 NNLO PDFs. The exact NLO results are shown with scale and PDF uncertainties while the approximate NNLO results include kinematics, scale, and PDF uncertainties.

the mass dependence at the LHC is smaller than at the Tevatron since we are further from production threshold here.

In Fig. 4, we show the LHC K factors as a function of mass for our central ($\mu = m$) cross sections calculated with the MRST 2006 NNLO (left) and CTEQ6.6M (right) PDFs. The LHC K factors are larger than those shown in Fig. 2. They are almost identical for the two sets and are virtually independent of mass. The approximate NNLO cross section is $\sim 8\%$ larger than the NLO cross section.

Finally, we provide predictions for the initial LHC run at $\sqrt{S} = 10$ TeV with $m = 172$ GeV. Using the MRST 2006 NNLO PDFs, the exact NLO cross section is $414 \pm 52 \pm 8$ pb while the NNLO approximate cross section is

$$\sigma_{pp \rightarrow t\bar{t}}^{\text{NNLOapprox}}(10 \text{ TeV}, m = 172 \text{ GeV}, \text{MRST}) = 446 \pm 3 \pm 9 \text{ pb} = 446 \pm 33 \text{ pb}. \quad (3.3)$$

With the CTEQ6.6M PDFs we find that the NLO cross section is $385 \pm 47 \pm 19$ pb and the NNLO approximate cross section is

$$\sigma_{pp \rightarrow t\bar{t}}^{\text{NNLOapprox}}(10 \text{ TeV}, m = 172 \text{ GeV}, \text{CTEQ}) = 415 \pm 2 \pm 20 \text{ pb} = 415 \pm 34 \text{ pb}. \quad (3.4)$$

CTEQ6.6M		
Mass (GeV)	$\sigma(\text{NLO} \pm \text{scale} \pm \text{PDF})$ (pb)	$\sigma(\text{NNLO approx} \pm \text{kinematics} \pm \text{scale} \pm \text{PDF})$ (pb)
165	1035 $^{+125}_{-121}$ $^{+31}_{-34}$	1114 ± 5 $^{+87}_{-55}$ $^{+33}_{-37}$
166	1007 $^{+121}_{-118}$ $^{+31}_{-33}$	1084 ± 5 $^{+84}_{-54}$ $^{+33}_{-35}$
167	979 $^{+117}_{-115}$ $^{+30}_{-33}$	1054 ± 5 $^{+81}_{-52}$ $^{+32}_{-35}$
168	952 $^{+114}_{-112}$ $^{+30}_{-32}$	1025 ± 5 $^{+79}_{-50}$ $^{+32}_{-34}$
169	927 $^{+110}_{-109}$ $^{+29}_{-31}$	997 ± 4 $^{+76}_{-49}$ $^{+31}_{-33}$
170	902 $^{+107}_{-106}$ $^{+29}_{-30}$	970 ± 4 $^{+74}_{-48}$ $^{+31}_{-32}$
171	877 $^{+105}_{-103}$ $^{+28}_{-29}$	944 ± 4 $^{+72}_{-47}$ $^{+30}_{-31}$
172	854 $^{+102}_{-100}$ $^{+27}_{-29}$	919 ± 4 $^{+70}_{-45}$ $^{+29}_{-31}$
173	831 $^{+99}_{-97}$ $^{+27}_{-29}$	894 ± 4 $^{+68}_{-44}$ $^{+29}_{-31}$
174	809 $^{+96}_{-95}$ $^{+26}_{-28}$	870 ± 4 $^{+66}_{-43}$ $^{+28}_{-30}$
175	788 $^{+94}_{-92}$ $^{+26}_{-27}$	847 ± 4 $^{+64}_{-42}$ $^{+28}_{-29}$
176	767 $^{+91}_{-90}$ $^{+25}_{-27}$	825 ± 4 $^{+62}_{-41}$ $^{+27}_{-29}$
177	747 $^{+89}_{-88}$ $^{+25}_{-26}$	803 ± 4 $^{+60}_{-39}$ $^{+27}_{-28}$
178	727 $^{+86}_{-85}$ $^{+25}_{-26}$	782 ± 4 $^{+59}_{-38}$ $^{+27}_{-28}$
179	709 $^{+84}_{-83}$ $^{+24}_{-25}$	762 ± 3 $^{+57}_{-37}$ $^{+26}_{-27}$
180	690 $^{+82}_{-81}$ $^{+23}_{-25}$	742 ± 3 $^{+55}_{-36}$ $^{+25}_{-27}$

Table 4: The $t\bar{t}$ production cross section in pp collisions at the LHC with $\sqrt{S} = 14$ TeV using the CTEQ6.6M PDFs. The exact NLO results are shown with scale and PDF uncertainties while the approximate NNLO results include kinematics, scale, and PDF uncertainties.

4 Conclusions

We have studied top quark production at the Tevatron and the LHC. Our work is the only calculation that employs full kinematics in the double differential cross section beyond NLL using the soft anomalous dimension matrix. We presented detailed results for the exact NLO and approximate NNLO $t\bar{t}$ cross sections at the Tevatron and the LHC for a wide range of top quark masses using the MRST 2006 NNLO and the CTEQ6.6M PDFs. The approximate NNLO corrections include soft-gluon contributions which significantly enhance the cross section. We find that further two-loop soft gluon contributions are expected to be negligible. We also included subleading Coulomb contributions and found them negligible at the Tevatron and very small at the LHC.

We provided detailed results for the theoretical uncertainties, including the kinematics ambiguity, scale variation, and PDF uncertainties. We found that the NNLO scale uncertainty is drastically reduced relative to NLO at the Tevatron where the kinematics uncertainty is larger. The PDF uncertainty is quite significant, especially for the CTEQ6.6M PDFs. At the LHC, the kinematics ambiguity is small. The NNLO scale variation is larger despite being significantly smaller than at NLO. The PDF uncertainty is smaller at the LHC than at the Tevatron. The results using the MRST 2006 NNLO and CTEQ6.6M PDFs are quite different from each other at both Tevatron and LHC energies.

Ongoing work with two-loop soft anomalous dimensions in the eikonal approximation [17] and recent analytical two-loop pieces of the NNLO corrections [24] promise further progress in the future.

Acknowledgements

The work of N.K. was supported by the National Science Foundation under Grant No. PHY 0555372. The work of R.V. was performed under the auspices of the U.S. Department of Energy by Lawrence Livermore National Security, LLC, Lawrence Livermore National Laboratory under Contract DE-AC52-07NA27344 and also supported in part by the National Science Foundation Grant NSF PHY-0555660.

References

- [1] CDF Collaboration, F. Abe *et al.*, Phys. Rev. Lett. **74**, 2626 (1995) [hep-ex/9503002]; D0 Collaboration, S. Abachi *et al.*, Phys. Rev. Lett. **74**, 2632 (1995) [hep-ex/9503003].
- [2] Tevatron Electroweak Working Group for CDF and D0, arXiv:0803.1683 [hep-ex].
- [3] CDF Collaboration, Phys. Rev. Lett. **96**, 202002 (2006) [hep-ex/0603043]; Phys. Rev. D **74**, 072006 (2006) [hep-ex/0607035]; Phys. Rev. D **74**, 072005 (2006) [hep-ex/0607095]; Phys. Rev. D **76**, 072009 (2007), arXiv:0706.3790 [hep-ex].
- [4] D0 Collaboration, Phys. Rev. D **74**, 112004 (2006) [hep-ex/0611002]; Phys. Rev. D **76**, 072007 (2007) [hep-ex/0612040]; Phys. Rev. D **76**, 092007 (2007), arXiv:0705.2788 [hep-ex]; Phys. Rev. D **76**, 052006 (2007), arXiv:0706.0458 [hep-ex]; arXiv:0803.2779 [hep-ex].
- [5] D0 Collaboration, V.M. Abazov *et al.*, Phys. Rev. Lett. **98**, 181802 (2007) [hep-ex/0612052]; arXiv:0803.0739 [hep-ex]; CDF Collaboration, Conf. Note 8964; Conf. Note 8968.
- [6] W. Wagner, Rept. Prog. Phys. **68**, 2409 (2005) [hep-ph/0507207]; A. Quadt, Eur. Phys. J. C **48**, 835 (2006); R. Kehoe, M. Narain, and A. Kumar, Int. J. Mod. Phys. A **23**, 353 (2008), arXiv:0712.2733 [hep-ex]; T. Han, arXiv:0804.3178 [hep-ph]; W. Bernreuther, arXiv:0805.1333 [hep-ph].
- [7] N. Kidonakis and G. Sterman, Phys. Lett. B **387**, 867 (1996); Nucl. Phys. **B505**, 321 (1997) [hep-ph/9705234].
- [8] N. Kidonakis, Phys. Rev. D **74**, 114012 (2006) [hep-ph/0609287]; Phys. Rev. D **75**, 071501(R) (2007) [hep-ph/0701080].
- [9] R. Bonciani, S. Catani, M.L. Mangano, and P. Nason, Nucl. Phys. **B529**, 424 (1998) [hep-ph/9801375].
- [10] G. Sterman and W. Vogelsang, JHEP **02**, 016 (2001) [hep-ph/0011289].

- [11] N. Kidonakis, Phys. Rev. D **64**, 014009 (2001) [hep-ph/0010002].
- [12] N. Kidonakis, E. Laenen, S. Moch, and R. Vogt, Phys. Rev. D **64**, 114001 (2001) [hep-ph/0105041].
- [13] M. Cacciari, S. Frixione, M.L. Mangano, P. Nason, and G. Ridolfi, arXiv:0804.2800 [hep-ph].
- [14] N. Kidonakis, Phys. Rev. D **73**, 034001 (2006) [hep-ph/0509079].
- [15] N. Kidonakis and R. Vogt, Phys. Rev. D **68**, 114014 (2003) [hep-ph/0308222].
- [16] S.M. Aybat, L.J. Dixon, and G. Sterman, Phys. Rev. Lett. **97**, 072001 (2006) [hep-ph/0606254]; Phys. Rev. **D74**, 074004 (2006) [hep-ph/0607309].
- [17] N. Kidonakis and P. Stephens, in *DIS 2008*, arXiv:0805.1193 [hep-ph].
- [18] J. Kodaira and L. Trentadue, Phys. Lett. **112B**, 66 (1982).
- [19] S. Moch and P. Uwer, arXiv:0804.1476 [hep-ph].
- [20] W. Bernreuther, R. Bonciani, T. Gehrmann, R. Heinesch, T. Leineweber, P. Mastrolia, and E. Remiddi, Nucl. Phys. **B706**, 245 (2005) [hep-ph/0406046].
- [21] P. Nason, S. Dawson, and R.K. Ellis, Nucl. Phys. **B303**, 607 (1988);
W. Beenakker, H. Kuijf, W.L. van Neerven, and J. Smith, Phys. Rev. D **40**, 54 (1989);
W. Beenakker, W.L. van Neerven, R. Meng, G.A. Schuler, and J. Smith, Nucl. Phys. **B351**, 507 (1991).
- [22] A.D. Martin, W.J. Stirling, R.S. Thorne, and G. Watt, Phys. Lett. B **652**, 292 (2007) [arXiv:0706.0459].
- [23] P.M. Nadolsky, H.-L. Lai, Q.-H. Cao, J. Huston, J. Pumplin, D. Stump, W.-K. Tung, and C.-P. Yuan, arXiv:0802.0007 [hep-ph].
- [24] M. Czakon, A. Mitov, and S. Moch, Phys. Lett. B **651**, 147 (2007), arXiv:0705.1975 [hep-ph]; Nucl. Phys. **B798**, 210 (2008), arXiv:0707.4139 [hep-ph]; M. Czakon, arXiv:0803.1400 [hep-ph].